

EFFECT OF METAL OXIDE ON ANTI-MICROBIAL FINISHING OF COTTON FABRIC

Yin Ling Lam,^{a,*} Chi Wai Kan, and Chun Wah M. Yuen^a

Cellulosic fibres provide a very agreeable environment for growth of bacteria due to large surfaces with high moisture absorbability. Therefore, the demand for an anti-microbial finish as an effective means of preventing disease transmission is high; it inhibits growth of or kills microorganisms on textile fabrics. This paper reports results of experiments where silver oxide (Ag₂O) or zinc oxide (ZnO) was used as a catalyst with the halogenated phenoxy compound (Microfresh, MF) and a binder (Microban, MB) on cotton fabrics to improve treatment effectiveness and minimize its side effects. Anti-microbial-treated fabrics showed some new characteristic peaks in chemical structure as evaluated by Fourier Transform Infrared Spectroscopy. In an anti-microbial test, it was found that anti-bacterial activity increased as MF-MB chemical agents were applied to the fabrics. A noticeable result was that the metal oxide catalyst had a significant effect on enhancing the performance. Surface morphology of anti-microbial-treated cotton specimens showed roughened and wrinkled fabric surface with high deposition of the finishing agent, which had a lower breaking load and tearing strength resulting from side effects of the acidic treatment. However, the addition of the Ag₂O catalyst was able to compensate for the reduction in tensile and tearing strength, and it is considered harmless for human skin.

Keywords: Antimicrobial; Cotton; Catalyst; Silver oxide; Zinc oxide

Contact information: a: Institute of Textiles and Clothing, The Hong Kong Polytechnic University, Hung Hom, Kowloon, Hong Kong, China; * Corresponding author: astroboyling@yahoo.com

INTRODUCTION

Cotton fabric is highly popular to society because of its excellent properties such as regeneration, bio-degradation, softness, affinity to skin, and sweat-absorbing properties (Zhang *et al.* 2009; Chen and Chiang 2008). However, cotton fabric is very prone to attack by certain microorganisms, insects, and fungi that cause functional, hygienic, and aesthetic difficulties (Chen and Burns 2006; Ramachandran *et al.* 2004; Daoud *et al.* 2005; El-Shishtawy *et al.* 2011; Gao and Cranston 2008; Gorenssek and Recelj 2007; Ilić *et al.* 2009; Abo-Shosha *et al.* 2007). Microbial infestation cannot be removed by even the most frequent washing, with the exception of washing at boiling temperature, which is not suitable (or practical) for textiles. Extensive efforts have been made to control infections caused by microorganisms and, therefore, a large demand exists for anti-microbially finished textiles capable of avoiding or limiting microbial fibre degradation, odor generation, as well as bacterial incidence and spread (Ramachandran *et al.* 2004; Mahltig *et al.* 2005; Parthasarathi and Borkar 2007; Rajendran *et al.* 2010;

Ibrahim *et al.* 2009; Ibrahim *et al.* 2010, 2012). There are three different methods of applying anti-microbial agents to textiles: (i) anti-bacterial agents are directly adsorbed onto fibres; (ii) anti-bacterial agents are confined in the network structure of a reactive synthetic resin formed on the fibre surface; and (iii) anti-bacterial agents are covalently bounded to cellulosic fibres (Nakashima *et al.* 2001). In the first method, despite easy application, agents applied can be lost during laundering. The last two methods have high durability against laundering; however they require heavy equipment and complex procedures and are, therefore, costly (Nakashima *et al.* 2001).

Bacteria have different membrane structures classified as Gram negative or Gram positive (Morones *et al.* 2005). Gram negative bacteria exhibit only a thin peptidoglycan layer (around 2 to 3 nm) between the cytoplasmic membrane and the outer membrane, while Gram positive bacteria lack the outer membrane but have a peptidoglycan layer about 30 nm thick (Morones *et al.* 2005). Anti-microbial finishing can inhibit growth of or kill the invading bacteria in several ways, including (i) cell wall damage and/or inhibition of cell wall synthesis; (ii) changing the chemical or physical state of proteins and nucleic acid inside the cell; (iii) inhibition of enzymes inside the cell, thereby retarding normal biological activities and metabolism of the bacteria; and (iv) inhibition of synthesis of protein or nucleic acids, thereby interrupting the ability of the bacteria to grow and reproduce (Abo-Shosha *et al.* 2007).

Triclosan is a common anti-microbial agent and imparts durable anti-microbial efficacy to fabrics. Triclosan has anti-bacterial, anti-fungal, and anti-viral properties in the bisphenol group, which has hydroxyl-halogenated derivatives of two phenolic groups connected by various bridges, and exhibits a particular activity against Gram positive bacteria (Orhan *et al.* 2008). In order to improve the washing durability of anti-microbial finishing, aqueous application requires the use of dispersing agents and binders together with triclosan. Crosslinking agents are usually small molecules containing several functional groups capable of reacting with hydroxyl groups in cellulose (Orhan *et al.* 2008). When exposed to sunlight, triclosan breaks down into 2,8-dichlorodibenzo-p-dioxin which is a chemically related toxic polychlorinated dioxin. Owing to such health and environmental issues, a number of leading retailers as well as governments in Europe are concerned about or have banned the “unnecessary use” of triclosan in textiles and some other products (Gao *et al.* 2008).

In this paper, silver oxide (Ag_2O) or zinc oxide (ZnO) was used as a catalyst in the anti-microbial formulation (halogenated phenoxy compound, Microfresh Liquid Formulation 9200-200, MF) and a binder (polyurethane dispersion, Microban Liquid Formulation R10800-0, MB) was applied on cotton fabrics to improve treatment effectiveness and minimize the side effects.

EXPERIMENTAL

Materials

100% semi-bleached plain weave cotton fabric (58 ends/cm, yarn count 40 tex, in warp; 58 picks/cm, yarn count 38 tex, in weft; fabric weight 175g/m^2), of size 30 cm x 30 cm was used. The antimicrobial finishing agent and binder used were a halogenated

phenoxy compound (Microfresh Liquid Formulation 9200-200, MF) and polyurethane dispersion (Microban Liquid Formulation R10800-0, MB), respectively. The catalysts used were silver oxide (Ag_2O , 2 μm diameter), obtained from Sigma-Aldrich Co., having purity of 99.0+%, micro-zinc oxide (ZnO , 2 μm diameter), and nano-zinc oxide (nano- ZnO , 100 nm diameter) obtained from Fluka Chemical Corp. and Sigma-Aldrich Co. respectively, both having purity of 99+%. All other chemicals used in the study were reagent grade.

Antimicrobial Two-bath Pad-dry-cure Treatment

Cotton fabric samples were treated with different compositions of finishing agents as shown in Table 1. A two-bath method was used for the treatments. In the first bath, the fabrics were dipped and padded with antimicrobial agents (MF+MB) until wet pick up of 80% was achieved at 25°C. The fabrics were then dried at 140°C for 5 minutes. In the second bath, dipping and padding processes (80% wet pick up) were performed, using Ag_2O , ZnO , or nano- ZnO solution dispersed in 10% Matexil DN-VL (dispersing agent). Subsequently, padded fabrics were dried at 140°C for 5 minutes. Finally, the fabrics were conditioned at $21\pm 1^\circ\text{C}$ and $65\pm 5\%$ relative humidity for 24 hours, prior to any further treatment.

Table 1. Antimicrobial Treatment Conditions

Sample Symbol	Concentrations of agents				
	Microfresh	Microban	Zinc Oxide	Nano-Zinc Oxide	Silver Oxide
M1	0.25%	0.5%			
M2	0.25%	0.5%	0.1%		
M3	0.25%	0.5%	0.2%		
M4	0.25%	0.5%		0.1%	
M5	0.25%	0.5%		0.2%	
M6	0.25%	0.5%			0.1%
M7	0.25%	0.5%			0.2%
M8			0.1%		
M9			0.2%		
M10				0.1%	
M11				0.2%	
M12					0.1%
M13					0.2%

* Concentration percentage measured based on weight of volume.

Scanning Electron Microscopy (SEM)

Surface morphology of cotton fibres was examined by the JEOL JSM-6490 Scanning Electron Microscope, with an accelerating voltage of 20kV and a current of 10 μA at a high magnification power of up to 8000X.

Fourier Transform Infrared Spectroscopy (FTIR)

Chemical compositions of cotton specimens were studied with a Perkin Elmer Spectrum 100 of Fourier Transform Infrared spectrophotometer, with scanning range between 4000 and 700 cm^{-1} and attenuated total reflection (ATR). The average number of

scans was 128, and the area of the relevant signal in zero-order derivative spectrum was measured.

Antibacterial Activity

The size of the zone of inhibition/clearance and narrowing of streaks caused by the presence of the anti-bacterial agent permit an estimate of residual anti-bacterial activity of treated fabrics. In the agar diffusion method, the bacteria (K-12, *E. coli* non-pathogenic) was mixed with molten top broth agar at 60 °C and then plated on hardened Luria-Bertani (LB) agar. When the top agar was hardened, autoclaved textile samples were placed on the hardened LB agar in triplicate. After incubation at 37 °C overnight, plates were examined. Any observable zone of clearance (ZOC) was defined as growth inhibition of K-12 *E. coli* bacteria. The parallel streak method is a relatively quick and easily executed qualitative method to determine anti-bacterial activity of diffusible anti-microbial agents on treated textile materials with respect to the AATCC 147-2004 standard. Specimens of the test material with size of 25 mm x 50 mm, including the corresponding untreated control specimen of the same material, were placed in intimate contact with nutrient agar, which had been previously streaked with an inoculum of a test bacterium, *Staphylococcus aureus* (*S. aureus*). After incubation, a clear area (the zone of inhibition) of interrupted growth underneath and along the sides of the test material indicates anti-bacterial activity on the specimen.

Biological Safety Test

A cytotoxicity test was performed to evaluate biological safety of antimicrobial agents (MF and MB) and catalyst solution (Ag_2O , ZnO, and nano-ZnO). It was measured by 3-(4,5-dimethylthiazol-2-yl)-2,5-diphenyltetrazolium bromide, *i.e.* a tetrazole (MTS) assay. This is a standard test used for measuring the activity of enzymes that can reduce MTS to formazan, generating a purple color. When the amount of purple formazan produced by the cells treated with a test solution was compared with the amount of formazan produced by cisplatin (CDDP), effectiveness of the test solution in causing death or changing metabolism of cells can be deduced.

Grab Test

Tensile properties were measured in accordance with the ASTM D5034 – 95 standard using the constant-rate-of-extension (CRE) Instron 4411 tensile testing machine.

Elmendorf Tearing Test

Tearing strength was measured with an Elmendorf Tearing Tester manufactured by the Thwing-Albert Instrument Co., according to the ASTM D1424 – 96 standard.

RESULTS AND DISCUSSION

Morphological Study

The morphological structure of the control sample exhibited natural folds running parallel to the fibre axis. The fibre surface might be described as a smooth surface with

normal spiral structure (Fig. 1a). On the other hand, Fig.1b shows the SEM image of a cotton sample treated with 0.25% MF and 0.5% MB at a magnification of 3000X. When compared with Fig. 1a, the morphological structure of the MF-MB-treated specimen shows a rougher and more wrinkled fibre surface. Deposition of the finishing agent (by the binder) on the fibres damaged its surface due to the slight acidity in the agents, *i.e.* pH 5, as measured. The results indicated that cross-linking might play an important role in coating the cotton surface with anti-microbial agents because of formation of chemical bonding.

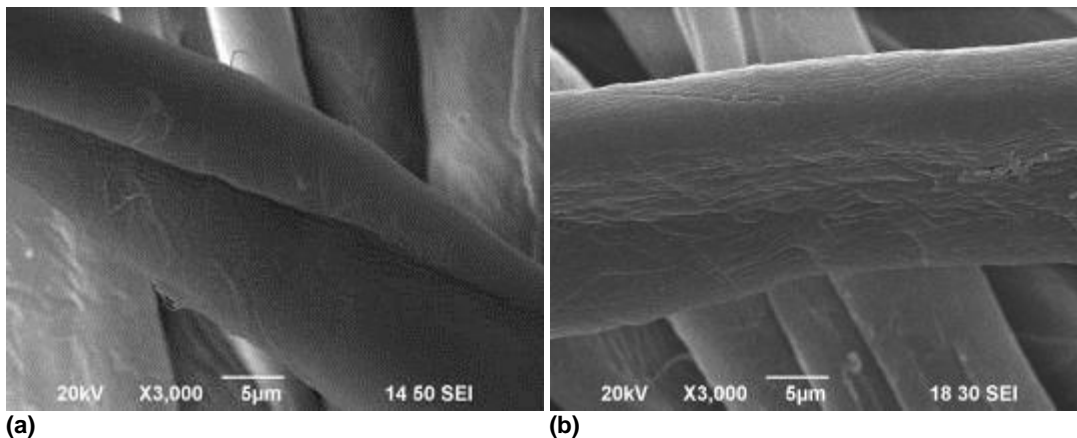


Fig. 1. SEM image of (a) control, (b) M1 specimen at 3000X

Figures 2a to 2c depict SEM images of the cotton specimen treated with 0.25% MF and 0.5% MB in the presence of 0.2% ZnO, nano-ZnO, and Ag₂O. Figures 2a and 2b show that the irregular-shaped ZnO and nano-ZnO particles were agglomerated and attached to the cotton fabric during the padding process. On the other hand, Ag₂O particles were not clearly shown in SEM images at a magnification of 3000X. High magnification SEM images, showing the existence of metal oxides, are depicted in Figs. 3a to 3c. Figures 3a and 3b clearly show that clustered ZnO and nano-ZnO particles were unevenly distributed on the fibre surface or between the fibres and the size of these particles varied slightly. ZnO and nano-ZnO agglomerated particles with diameters in the range of 0.35 to 1.50 µm and 0.05 to 1.25 µm, respectively, were observed. Agglomeration of particles was observed mainly due to the attraction between small particles on the surface. In addition, Fig. 3c illustrates that Ag₂O particles were attached on the fibre surface, while only the existence of small agglomerated particles was observable, *i.e.* the particles (diameters 0.23 to 0.63µm) were being agglomerated together.

Chemical Structure Analysis

FTIR-ATR analysis was performed on the control cotton fabric, as illustrated in Figs. 4a-f. The characteristic bands related to cellulose structure of cotton fibres were the hydrogen bonded OH stretching centered at 3300 cm⁻¹, the CO stretching centered at 1030 cm⁻¹, the CH stretching centered at 2900 cm⁻¹, and the CH wagging centered at 1310 cm⁻¹ (Karahan and Özdoğan 2008; Chung *et al.* 2004; Hartzell-Lawson and Hsieh 2000). In addition, the peak at around 1640 cm⁻¹ corresponded to the absorbed water molecules (Karahan and Özdoğan 2008; Chung *et al.* 2004)

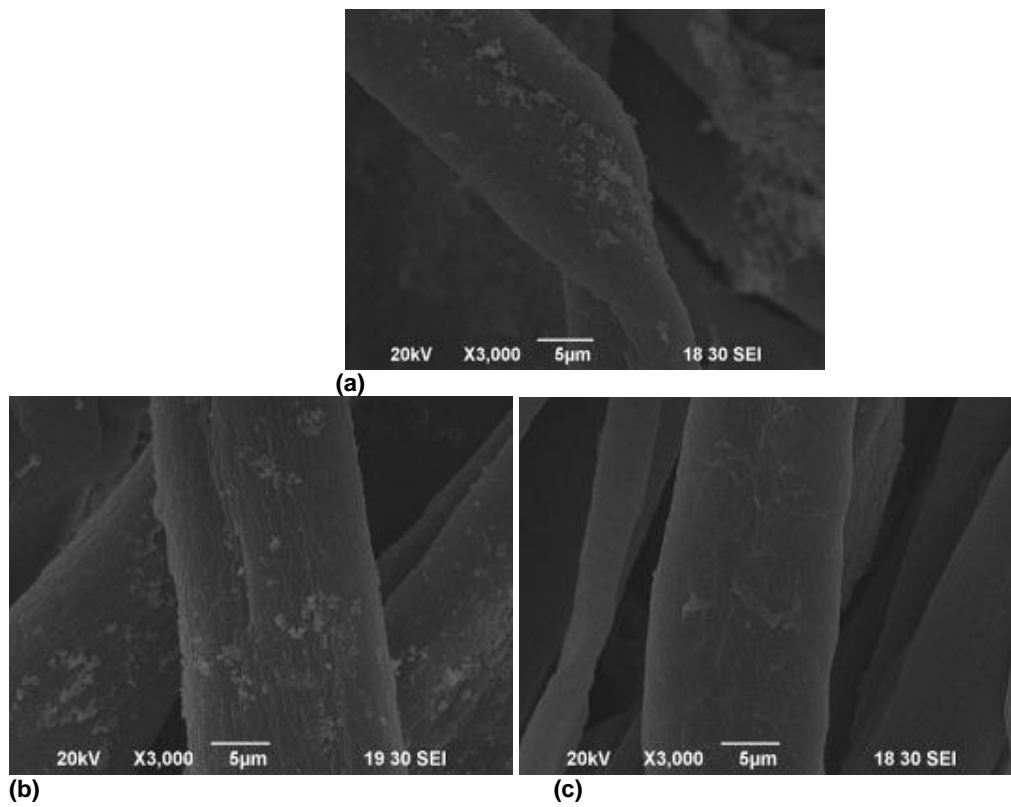


Fig. 2. SEM image of (a) M3, (b) M5, (c) M7 specimen at 3000X

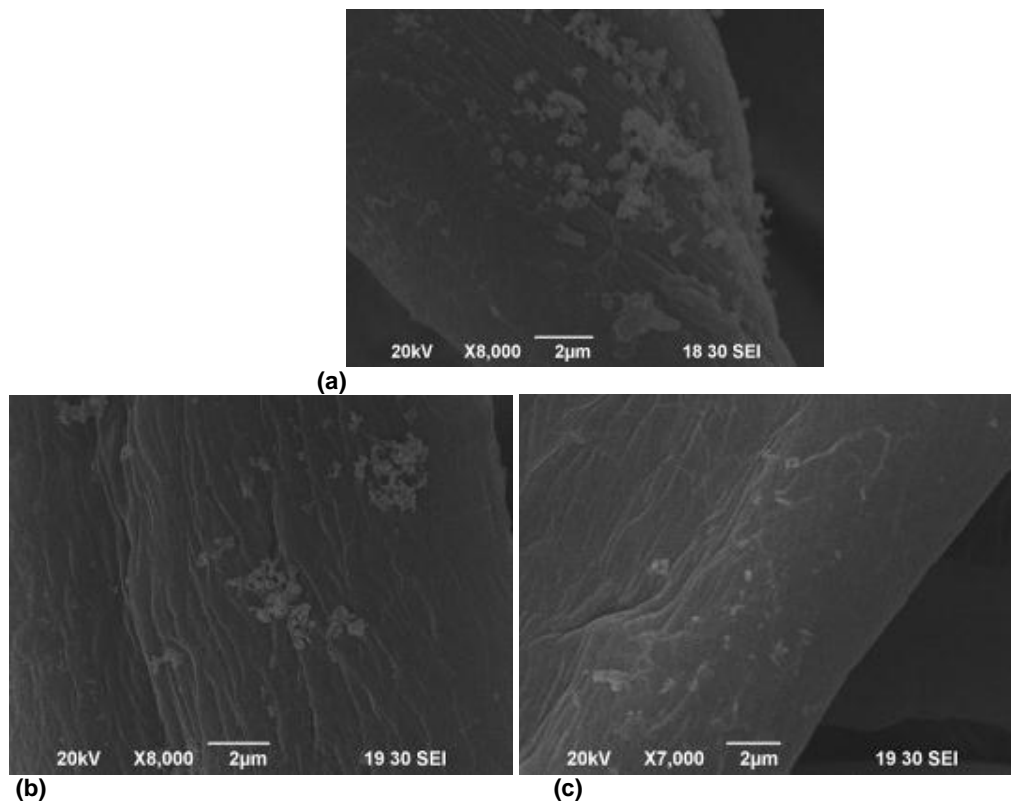
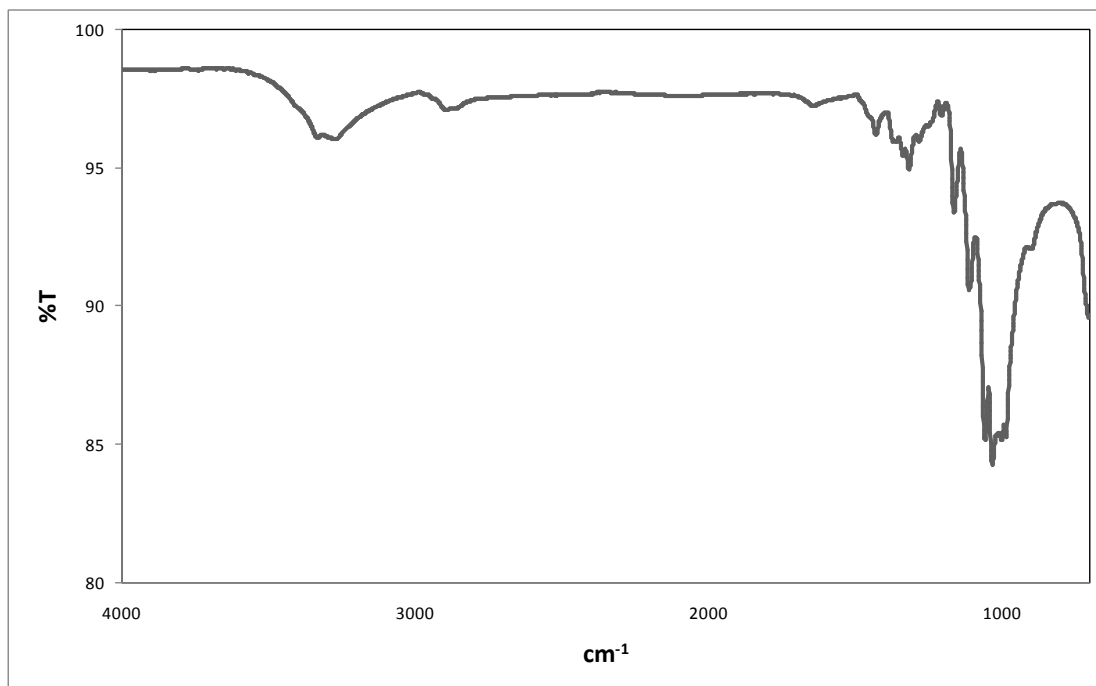
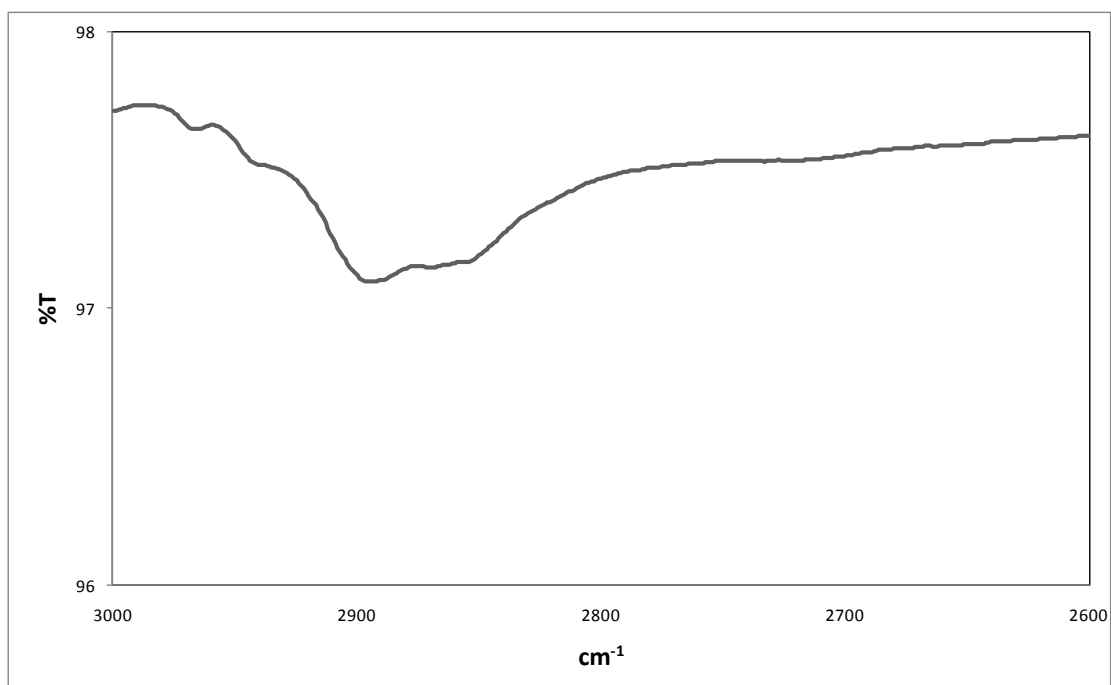


Fig. 3. SEM image of (a) M3, (b) M5, (c) M7 specimen at 7000-8000X

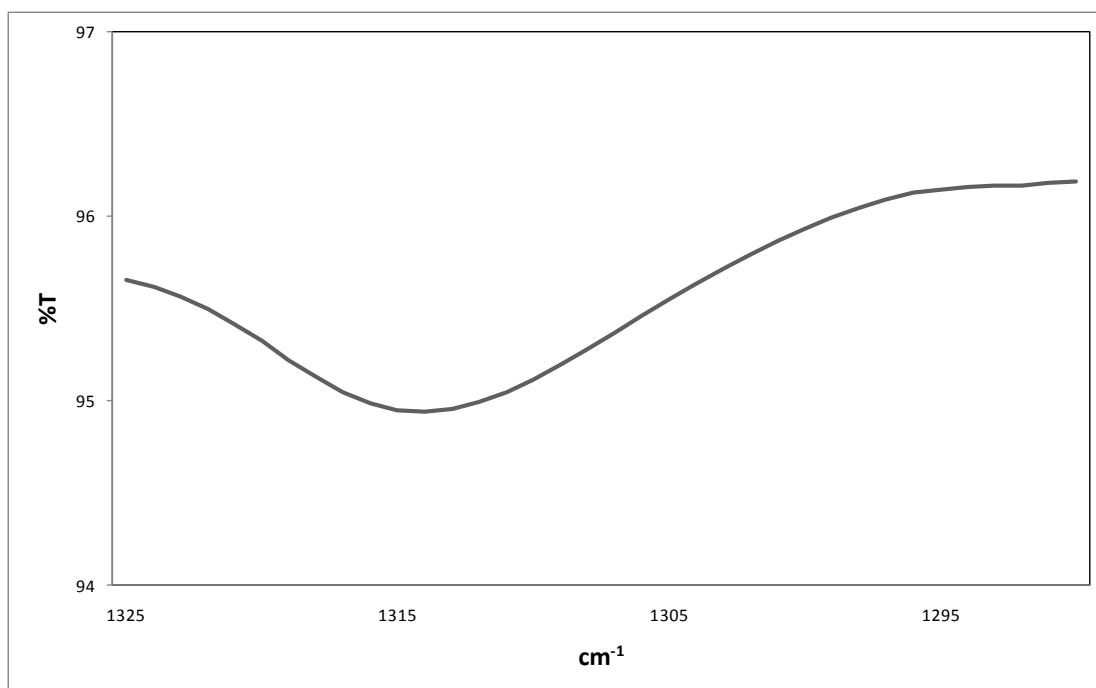


(a)

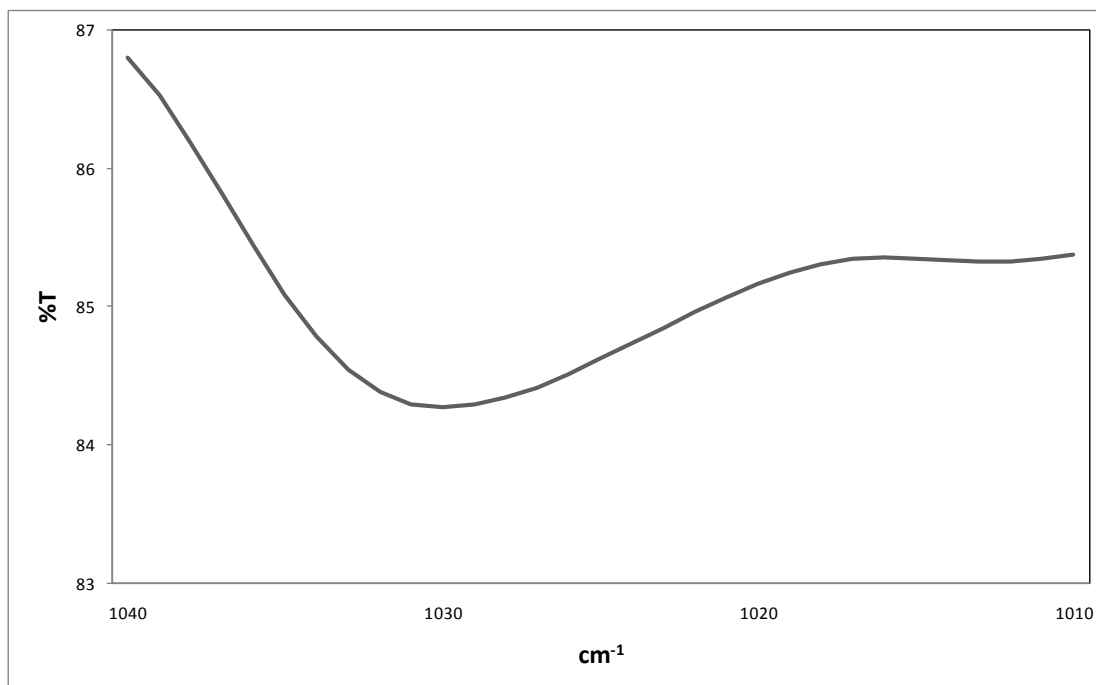


(b)

Fig. 4. (a) and (b): FTIR-ATR spectra of control cotton specimen at (a) 4000-700 cm⁻¹, (b) 3000-2600 cm⁻¹, (c) 1325-1290 cm⁻¹, (d) 1040-1010 cm⁻¹, (e) 3600-2900 cm⁻¹, (f) 1800-1500 cm⁻¹

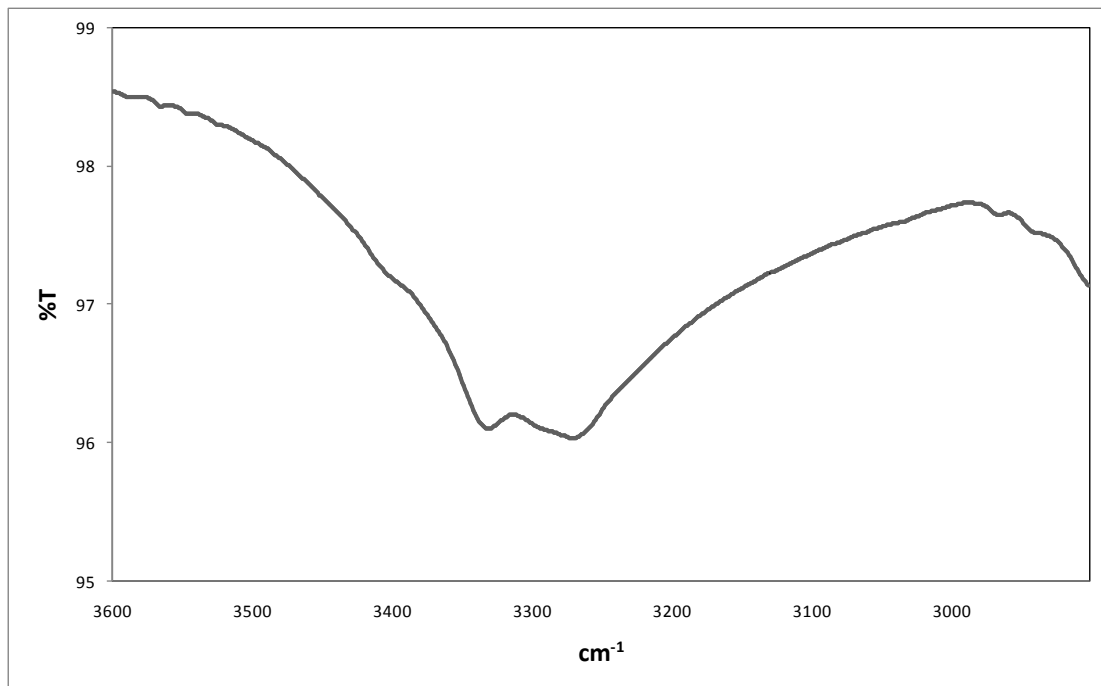


(c)

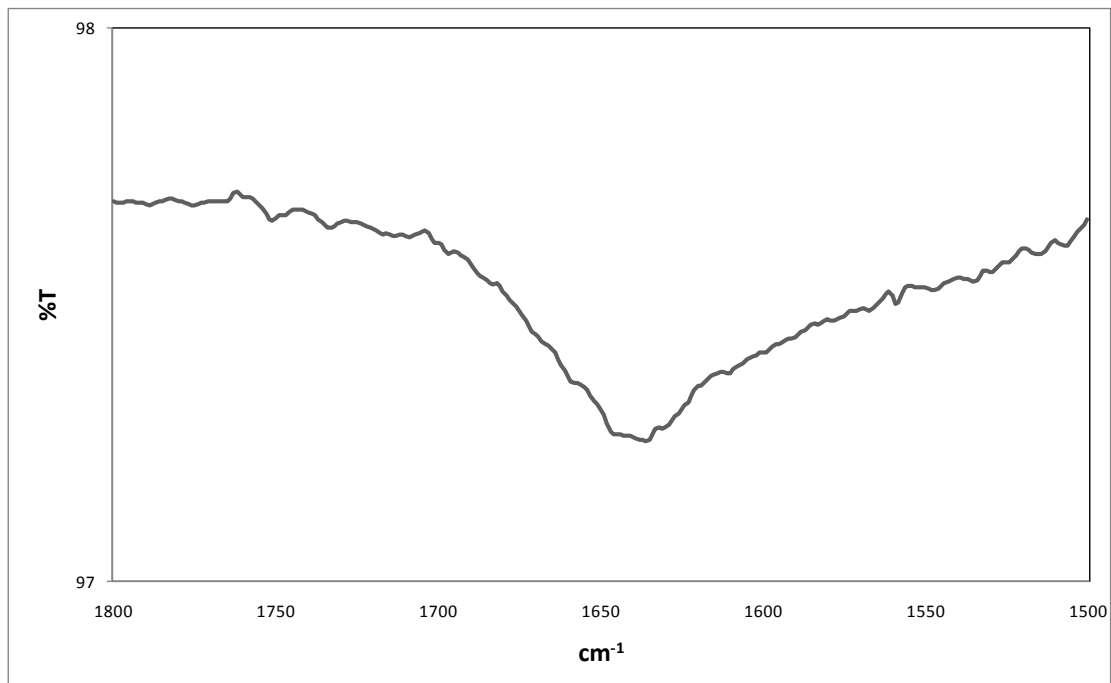


(d)

Fig. 4. (c and d): FTIR-ATR spectra of control cotton specimen at (a) 4000-700 cm^{-1} , (b) 3000-2600 cm^{-1} , (c) 1325-1290 cm^{-1} , (d) 1040-1010 cm^{-1} , (e) 3600-2900 cm^{-1} , (f) 1800-1500 cm^{-1}



(e)



(f)

Fig. 4. (e and f): FTIR-ATR spectra of control cotton specimen at (a) 4000-700 cm^{-1} , (b) 3000-2600 cm^{-1} , (c) 1325-1290 cm^{-1} , (d) 1040-1010 cm^{-1} , (e) 3600-2900 cm^{-1} , (f) 1800-1500 cm^{-1}

Microfresh Liquid Formulation 9200-200 contains triclosan, 2,4,4'-trichloro-2''-hydroxydiphenyl ether, as the active anti-microbial agent applied at the finishing stage or incorporated into the fibre during extrusion. Triclosan is very effective against a broad range of microorganisms, including antibiotic-resistant bacteria (Simoncic and Tomsic 2010). It connects the terminal hydroxyl group in each triclosan molecule to cellulose. However, the bonding is relatively weak (Simoncic and Tomsic 2010; Yazdankhah *et al.* 2006) and, therefore, triclosan has been applied to cellulosic fibres in combination with a binder to enhance washing durability of the anti-microbial coating. When metal oxides were added in the treatment, the triclosan molecules were catalyzed, providing an alternative reaction pathway to the reaction product. It was proposed that the hydroxyl group of the anti-microbial agent could dissociate at ZnO or Ag₂O surface and form a hydroxyl molecule with a surface atom O_{lattice} (Fig. 5, Equation (1)) (Diebold 2003; Hadjiivanov and Klissurski 1996). Thus, the presence of ZnO or Ag₂O catalyst played an important role in the anti-microbial finish, assisting in effectively cross-linking the cellulose and the triclosan (Fig. 5, Equation (2)).

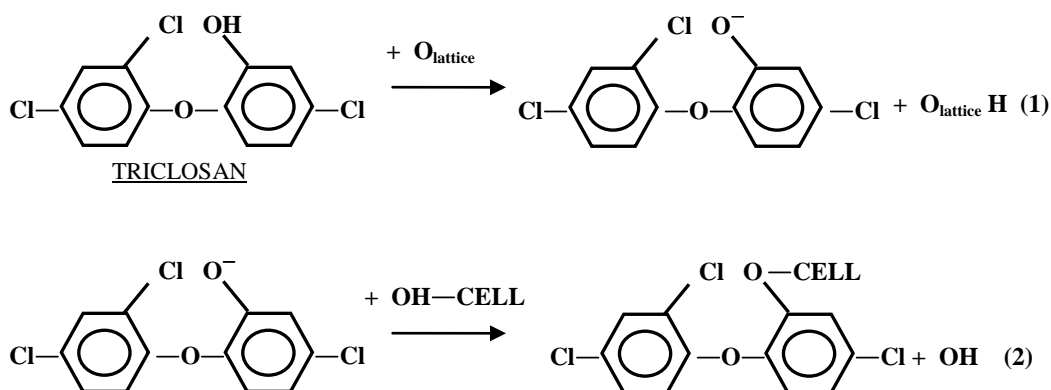
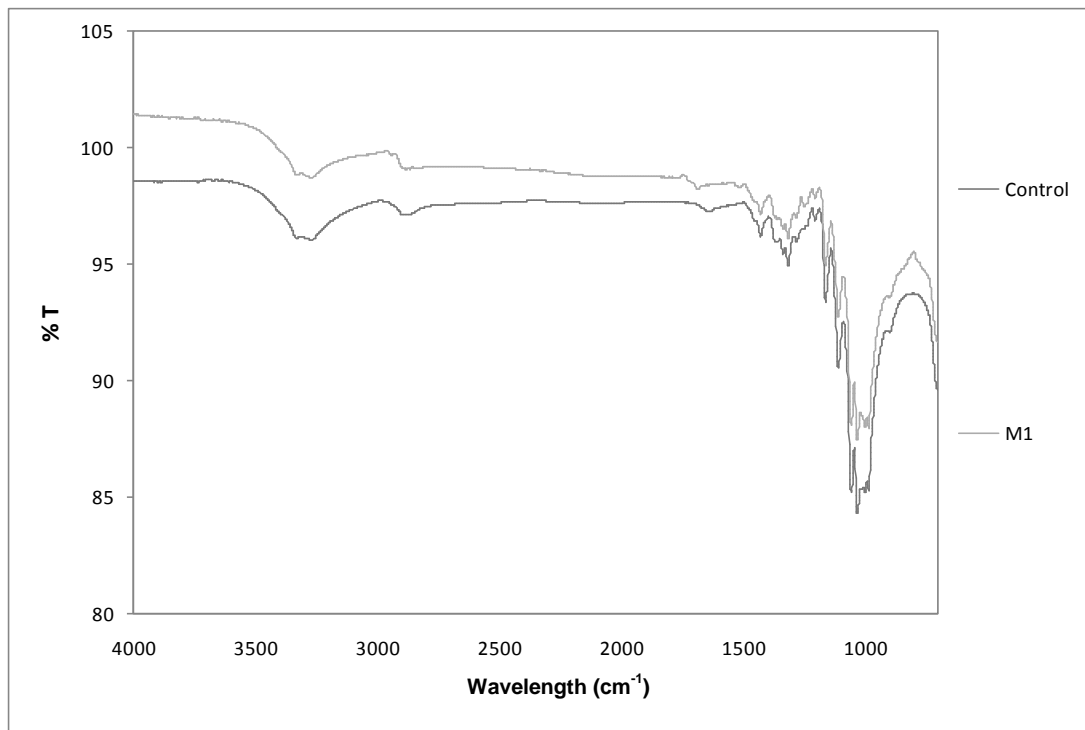


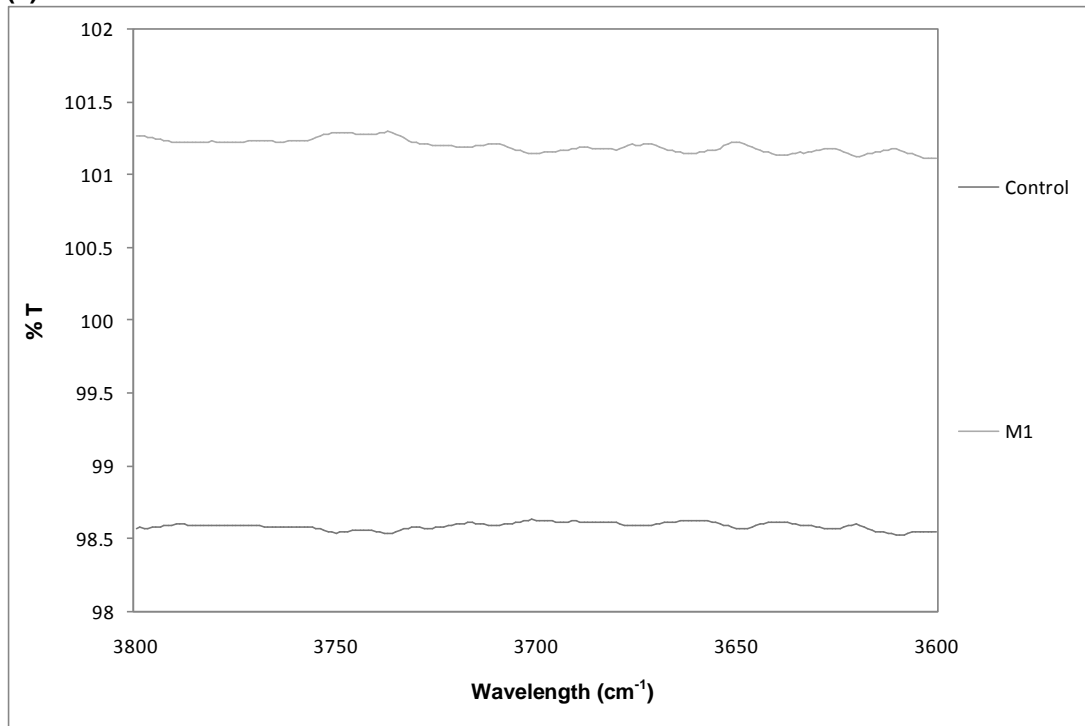
Fig. 5. Catalytic reaction between cellulose and triclosan

The FTIR-ATR spectra obtained from the control cotton fabric and MF-MB-treated fabric are depicted in Figs. 6a – 6d (full spectrum at 4000 to 700 cm⁻¹ is shown in Fig. 6a). It was proposed that there were strong hydroxyl stretching bands at 3700-3600 cm⁻¹ and 3420-3250 cm⁻¹ (Chalmers and Griffiths 2002), representing the presence of triclosan on the fabrics. However, the terminal hydroxyl group in triclosan molecule might have reacted with cellulose and, therefore, there were no new characteristic peaks formed, as shown in Figs. 6b and 6c. On the other hand, Fig. 6d shows two medium sharp bands at 1670 and 1510 cm⁻¹, which are due to the benzene ring in aromatic compounds (Chalmers and Griffiths 2002). Therefore, it was confirmed that the MF agent applied was bonded with the cotton fabrics.

The FTIR-ATR spectra of MF-MB-treated fabrics in the presence or absence of metal oxide catalyst are presented in Figs. 7a to 7e. In general, the spectra, as shown in Fig. 7a, of metal oxide-coated cotton fabric (M3, M5 and M7 specimens) do not reveal new peaks (downward peaks) from the M1 specimen, which means there was no chemical bond formation on the surface of cotton fabrics with metal oxide (El-Shishtawy *et al.* 2011; Vigneshwaran *et al.* 2007).

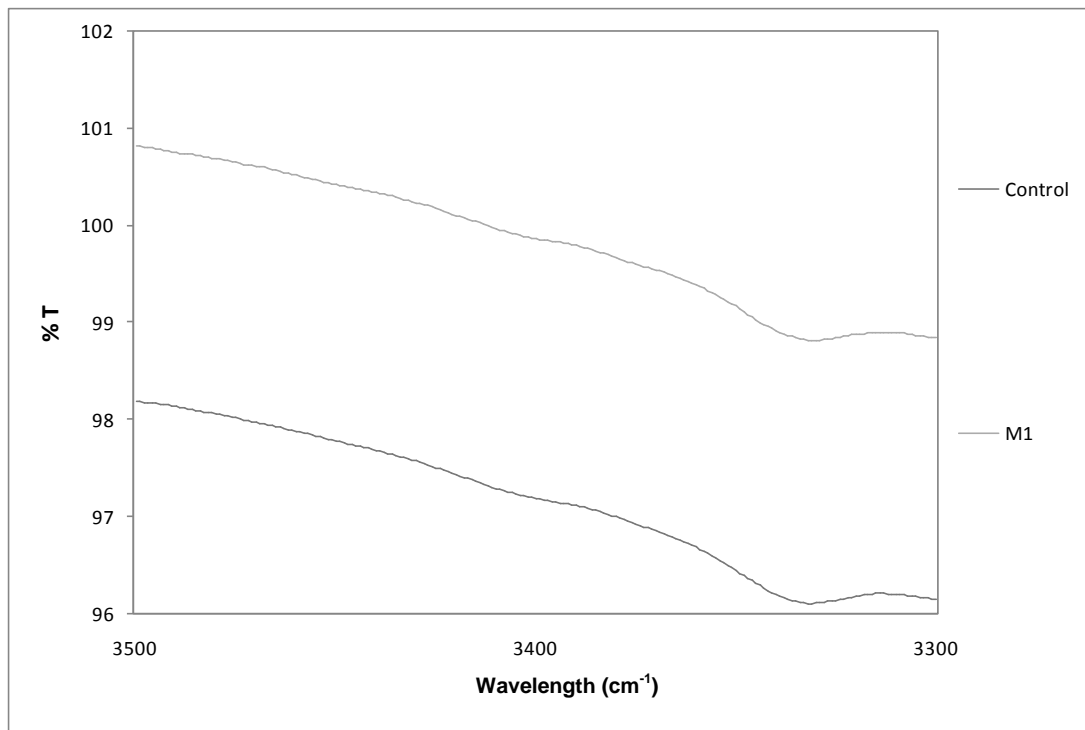


(a)

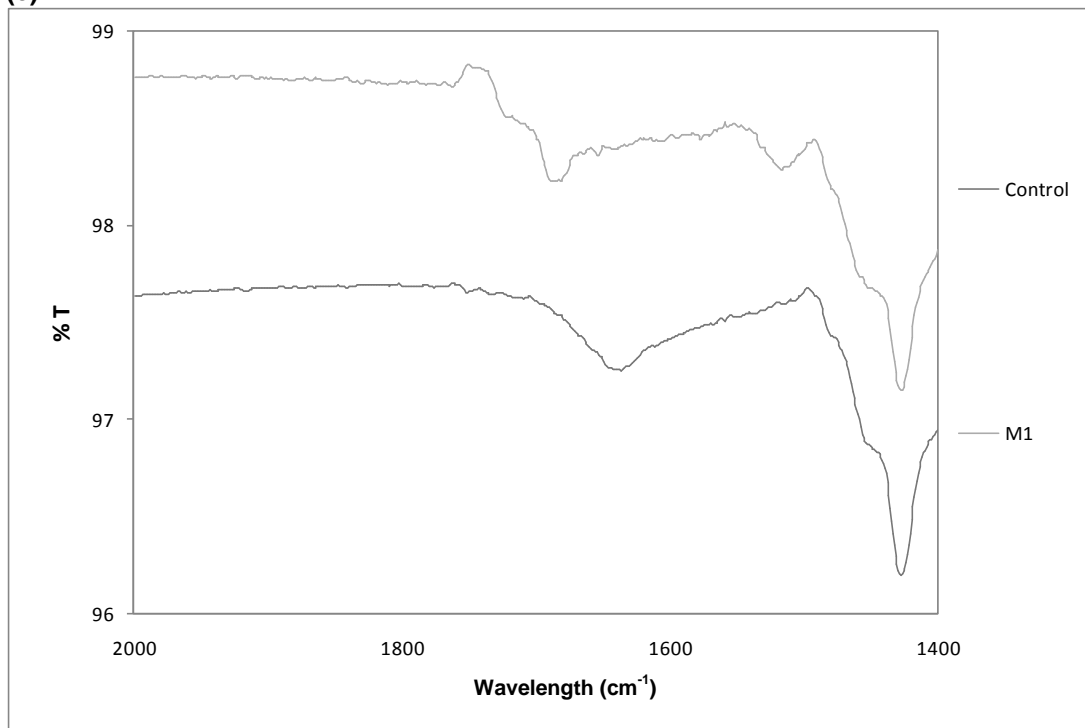


(b)

Fig. 6. (a and b): FTIR-ATR spectra of anti-microbial-treated cotton specimen at (a) 4000-700 cm⁻¹, (b) 3800-3600 cm⁻¹, (c) 3500-3300 cm⁻¹, (d) 2000-1400 cm⁻¹



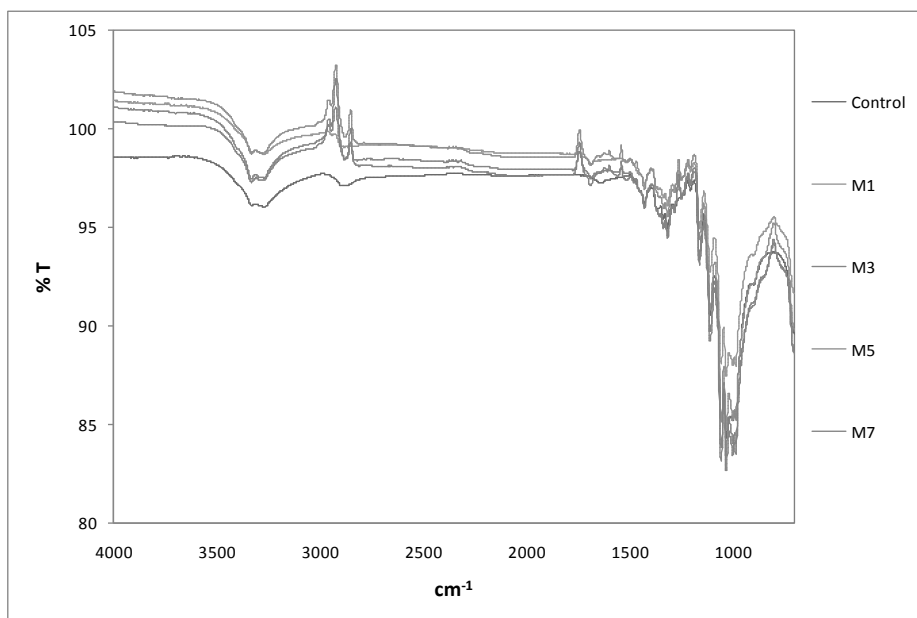
(c)



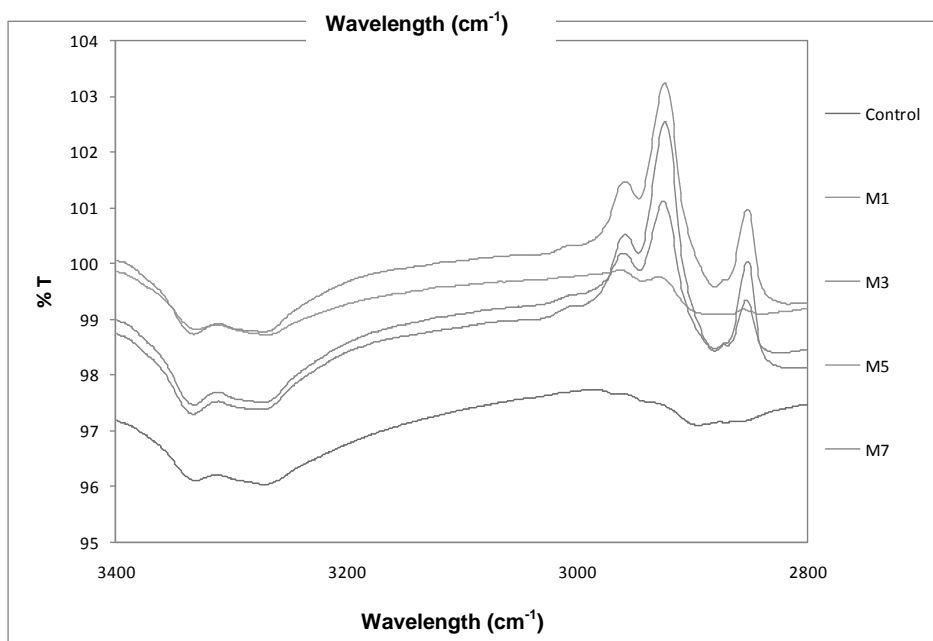
(d)

Fig. 6. (c and d): FTIR-ATR spectra of anti-microbial-treated cotton specimen at (a) 4000-700 cm^{-1} , (b) 3800-3600 cm^{-1} , (c) 3500-3300 cm^{-1} , (d) 2000-1400 cm^{-1}

The results further confirmed that metal oxide used in anti-microbial finishing worked as a catalyst. Furthermore, as shown in Figs. 7a – 7e, the spectra for M3, M5, and M7 specimens contained some signals that rose upward from the baseline. These signals are usually associated with water and carbon dioxide absorptions that have not been cancelled properly by the background spectrum. Nevertheless, the presence of water absorption might be due to the reaction between two hydroxyl groups formed when the O_{lattice} recovered to be metal oxide.

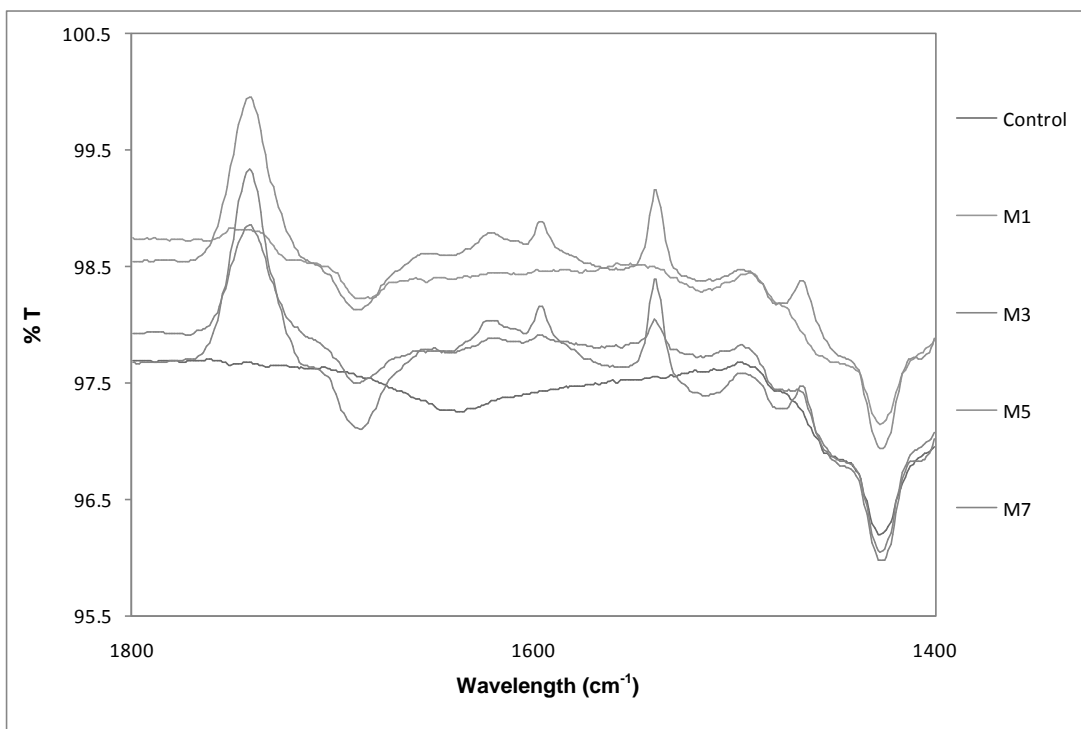


(a)

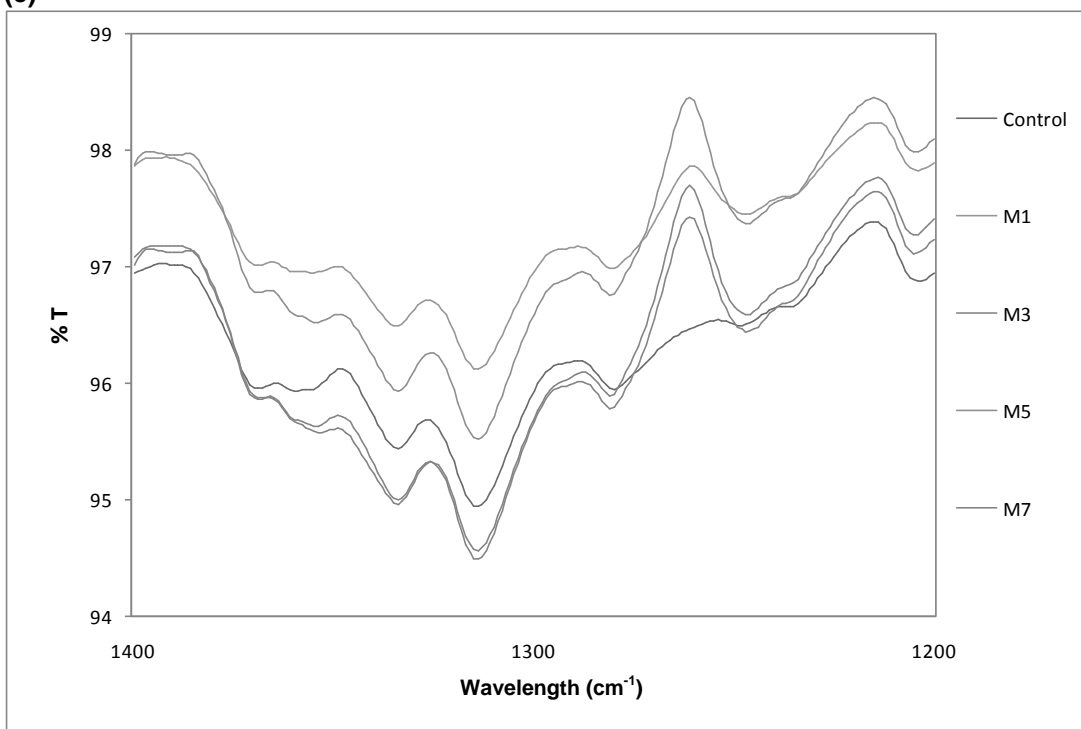


(b)

Fig. 7. FTIR-ATR spectra of anti-microbial-treated cotton specimen at (a) 4000-700 cm^{-1} , (b) 3400-2800 cm^{-1} , (c) 1800-1400 cm^{-1} , (d) 1400-1200 cm^{-1} , (e) 1000-700 cm^{-1}

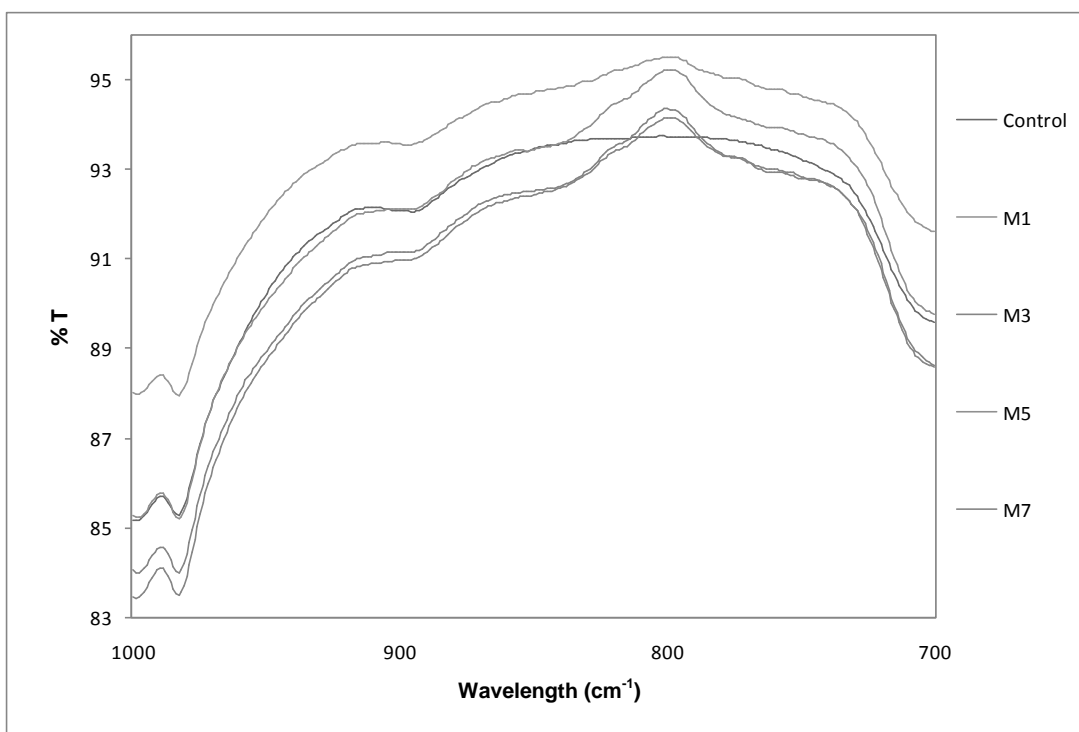


(c)



(d)

Fig. 7. (c and d): FTIR-ATR spectra of anti-microbial-treated cotton specimen at (a) 4000-700 cm^{-1} , (b) 3400-2800 cm^{-1} , (c) 1800-1400 cm^{-1} , (d) 1400-1200 cm^{-1} , (e) 1000-700 cm^{-1}



(e)

Fig. 7. (e): FTIR-ATR spectra of anti-microbial-treated cotton specimen at (a) 4000-700 cm^{-1} , (b) 3400-2800 cm^{-1} , (c) 1800-1400 cm^{-1} , (d) 1400-1200 cm^{-1} , (e) 1000-700 cm^{-1}

Anti-microbial Activity

This section reports results of anti-microbial properties of cotton fabric evaluated by both the agar diffusion method and the parallel streak method. By using the agar diffusion method, growth inhibition of Gram negative bacteria, *E. coli* (non-pathogenic), on untreated and anti-microbial-treated specimens was tested; *E. coli* was mixed with molten top broth agar and then plated on hardened Luria-Bertani (LB) agar with autoclaved specimens placed on it. After incubation at 37°C overnight, observable zone of clearance (ZOC), defined as growth inhibition of bacteria, was noticed in samples M1-M7, while control and M8-M13 specimens did not have anti-bacterial activity. The results found that 0.1 to 0.2% ZnO, nano-ZnO, or Ag₂O alone did not impart good anti-microbial properties against *E. coli* to cotton fabrics. In general, *E. coli* only has a thin layer of peptidoglycan (2 to 6 nm in thickness (Blake *et al.* 1999)), but a much more complex cell wall structure (6 to 18 nm in thickness (Blake *et al.* 1999)) with both an outer membrane and a plasma membrane (Fu *et al.* 2005; Page *et al.* 2007). Therefore, the additional outer membrane of the bacteria influences permeability of many molecules and makes it more resistant to many chemical agents (Fu *et al.* 2005; Page *et al.* 2007). Table 2 summarizes measured and averaged ZOC of M1-M7 treated specimens with respect to *E. coli*. The anti-microbial activity of M1 specimen, *i.e.* around 2 cm in ZOC, was contributed mainly by the MF agent, which might have been active at very low concentration. MF works with the concept of controlled release and provides a zone of inhibition (Yazdankhah *et al.* 2006; Orhan *et al.* 2008). It inhibits bacterial fatty acid bio-

synthesis (an important bio-synthesis to cell growth) at the enoyl-acyl carrier protein reductase (FabI enzyme) step, by formation of a ternary FabI- triclosan complex (Yazdankhah *et al.* 2006; Orhan *et al.* 2008; Stewart *et al.* 1999; Suller and Russell 2000; Heath *et al.* 1999). Once the membrane has been breached, no further significant obstacles block the approach of the radicals, and cell death can then occur.

Table 2. The Zone of Clearance (against *E. coli*) of Test Specimens

Sample Symbol	Mean zone of clearance (cm)
M1	2.0
M2	3.0
M3	2.0
M4	2.0
M5	2.0
M6	2.5
M7	2.5

In general, ZnO and Ag₂O have been found to have several advantages, including low toxicity and high efficiency in preventing infection (active oxygen species generated by the particles could be a mechanism) (Vigneshwaran *et al.* 2006). In addition, as discussed, the hydroxyl group of the MF agent can dissociate at ZnO or Ag₂O surface and form a hydroxyl molecule with a surface atom O_{lattice} assisting in effectively cross-linking the cellulose and the triclosan. Moreover, theoretically, nano-particles are supposed to have much higher activity than bulk particles (Rajendran *et al.* 2010). However, as shown in Table 2, only M2, M6, and M7 specimens showed bigger ZOC in comparison with the M1 specimen. As discussed in Section 3.1, metal oxides clustered in bigger particles due to instability of surface attraction between small particles, *i.e.* ZnO, nano-ZnO, and Ag₂O with diameters in the range of 0.35 to 1.50 μm, 0.05 to 1.25 μm, and 0.23 to 0.63 μm, respectively. Therefore, the results demonstrated that only relatively small clustered particles could provide a surface atom O_{lattice} effectively in the catalyzed reaction.

In this study, the parallel streak method was used to determine anti-bacterial activity of treated textile materials against Gram positive bacteria, *S. aureus*. During the test, specimens were placed in intimate contact with nutrient agar, previously streaked with an inoculum of *S. aureus*. After incubation, a clear area of interrupted growth underneath and along the sides of the test material indicated anti-bacterial activity on the specimen. Table 3 summarizes the mean clearance distance of the bacteria from the specimens. In general, *S. aureus* has a relatively thick wall (20 to 80 nm (Blake *et al.* 1999; Shrivastava *et al.* 2007)), which is composed of many layers of peptidoglycan polymer and one plasma membrane. These layers of peptidoglycan are composed of a fairly open network polymer of N-acetylmuramic acid and N-acetylglucosamine polysaccharide chains with peptide bridges (Fu *et al.* 2005; Page *et al.* 2007). Hence, the Gram positive bacteria are less resistant to many chemical agents than Gram negative cells (Fu *et al.* 2005). Table 3 shows that the control fabric inhibited the growth of *S. aureus* with an average of 1.2cm ZOC in the agar plate. This was because the semi-bleached control cotton fabrics might have contained some bleach residues; hydrogen peroxide (H₂O₂) was used to remove natural coloration and remaining trace impurities from the pre-finishing stage.

Table 3. The Mean Clearance Distance of the *S. aureus* Bacteria from the Specimens

Sample Symbol	Mean Clearance Distance (cm)
Control	1.2
M1	1.5 (+25%)
M2	1.9 (+58%)
M3	2.2 (+83%)
M4	2.0 (+67%)
M5	1.7 (+42%)
M6	1.7 (+42%)
M7	2.1 (+75%)
M8	1.2 (+0%)
M9	1.2 (+0%)
M10	0.9 (-25%)
M11	0.5 (-58%)
M12	0.0 (-100%)
M13	0.0 (-100%)

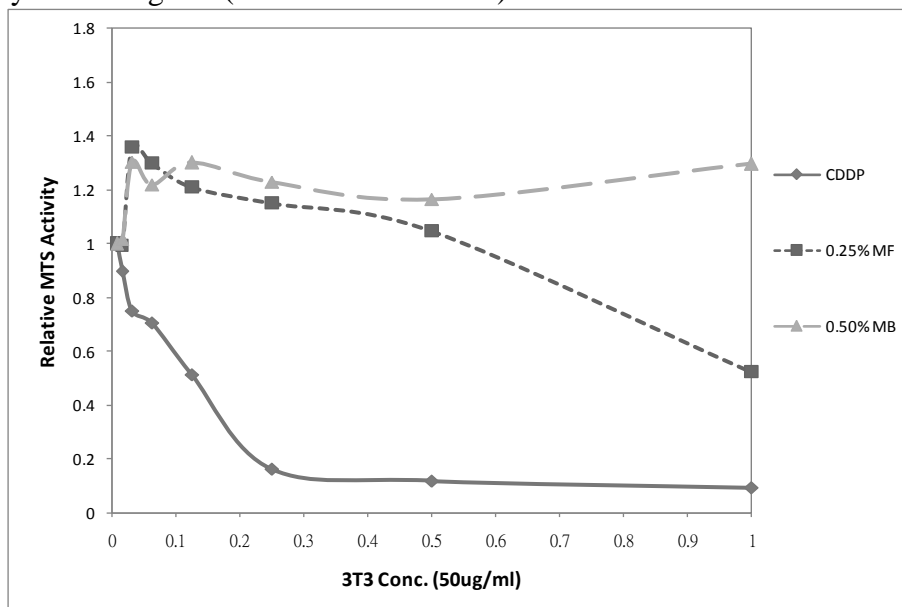
Although H₂O₂ is less harmful compared to other reactive oxygen species, such as hydroxyl radicals and superoxide ions, it can enter the cells and exhibit anti-bacterial activity (Blake *et al.* 1999; Fu *et al.* 2005). For M8-M13 specimens, the anti-bacterial activity dropped or remained unchanged because the small concentration of metal oxide itself could not exhibit good anti-microbial property on the fabrics and the wet padding process might have even washed out the bleach residues from the fabric surface.

At a very low concentration of MF, anti-bacterial activity on M1 specimen was enhanced, providing a slightly larger zone of inhibition compared to the control specimen. The result proved that the MF agent induced anti-microbial activity against Gram positive, as well as Gram negative bacteria. Moreover, according to Table 3, fabrics finished with MF-MB in the presence of metal oxide exhibited better anti-microbial activity and were more effective against *S. aureus* than *E. coli*. This is attributed to the fact that the *S. aureus* cell wall typically lacks the outer membrane as found in *E. coli* (Shrivastava *et al.* 2007). The results indicate that M3 and M7 specimens had over 75% increment in anti-microbial activity compared to the control fabric. An increase in anti-bacterial activity on increasing concentration of ZnO and Ag₂O in the medium occurred. On the other hand, the M4 specimen demonstrated better anti-microbial activity than the M5 specimen, as presented in Table 3.

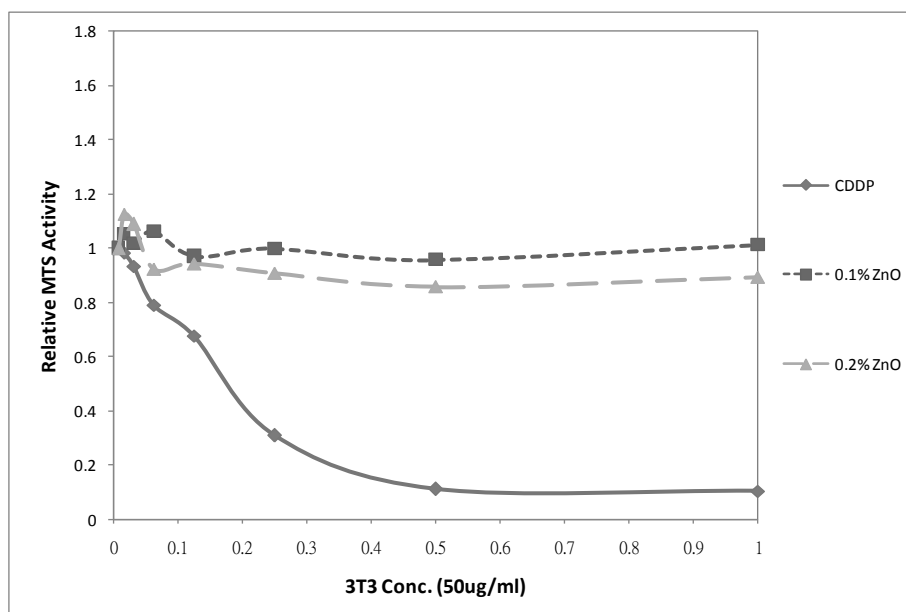
Generally speaking, it is believed that nano-particles release ions which react with thiol groups (-SH) of proteins present on the bacterial cell surface. Nano-particles inactivate the proteins and stop transportation of nutrients through the cell wall, thereby decreasing membrane permeability and eventually causing cell death (Rezaei-Zarchi *et al.* 2010; Zhang and Chen 2009; Holt and Bard 2005). However, as discussed, nano-ZnO clustered in bigger particles due to instability of surface attraction between small particles, *i.e.* higher concentrations of nano-particles cause greater agglomeration of the particles. Therefore, the results demonstrated that only relatively small clustered nano-particles, *i.e.* at 0.1% concentration, gave better results.

Cytotoxicity Test (MTS assay)

Since the anti-bacterial effect might be related to a wide spectrum of cellular toxicity, activities of fibroblast-like cells cultured in the presence of MF, MB, and metal oxides were explored. Figures 8a to 8d demonstrate results of the cytotoxicity test, using a fibroblast cell line (NIH 3T3), which is commonly found in skin and other connective tissues. Every plotted point on the lines came from triple runs of each concentration of the test agents. The drop of relative 3-(4,5-dimethylthiazol-2-yl)-2,5-diphenyltetrazolium bromide, *i.e.* a tetrazole (MTS) activity in the Y-axis, indicated the extent of cell death induced by the test agents (Lewinski *et al.* 2008).

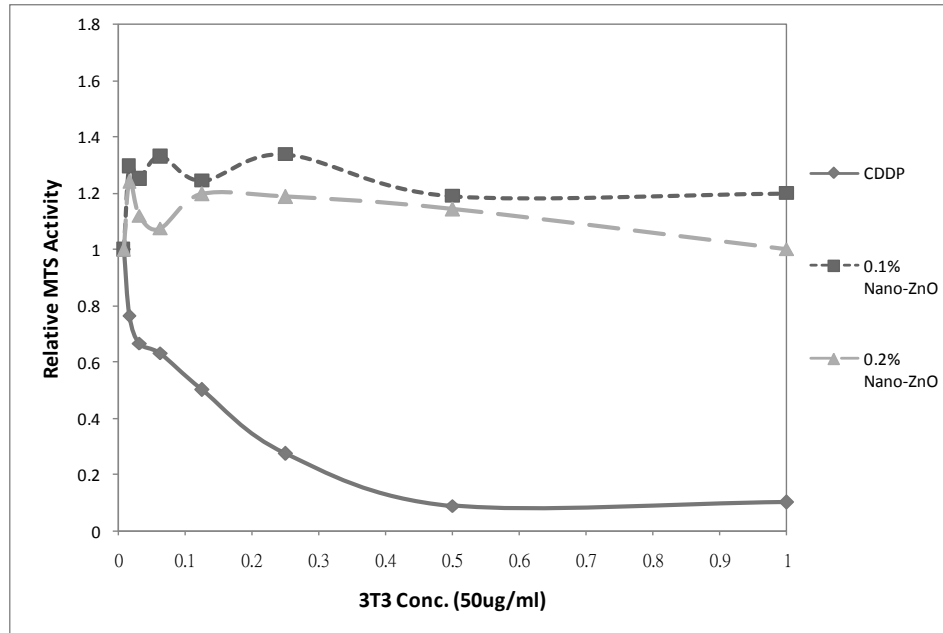


(a)

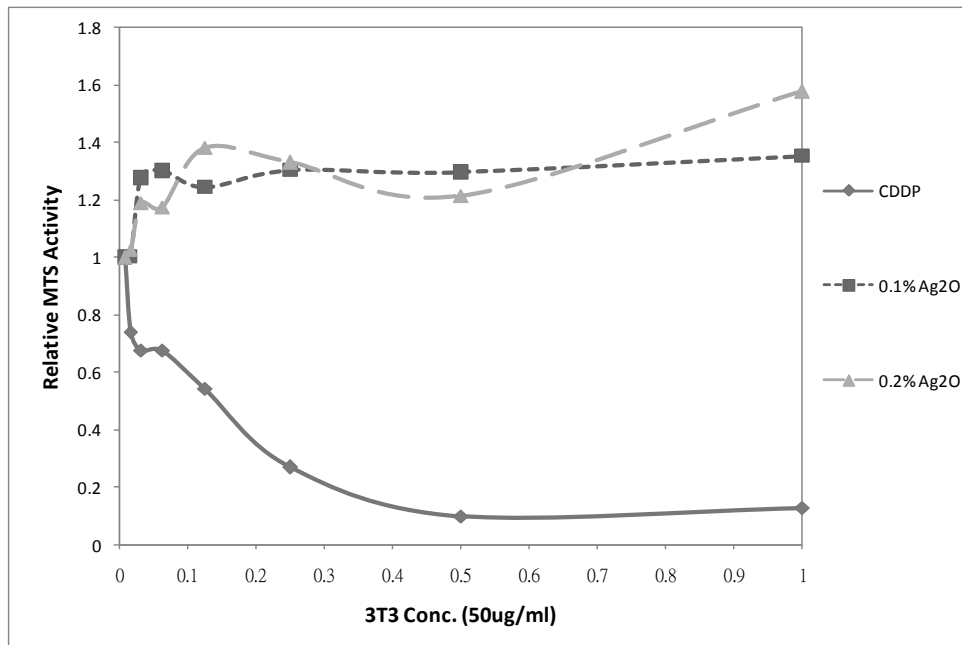


(b)

Fig. 8. (a and b): Cytotoxicity test result of (a) MF and MB, (b) ZnO, (c) nano-ZnO, (d) Ag₂O



(c)



(d)

Fig. 8. (c and d): Cytotoxicity test result of (a) MF and MB, (b) ZnO, (c) nano-ZnO, (d) Ag₂O

Viability assays are vital steps in toxicology that explain the cellular response to a toxicant, which may give information on cell death, survival, and metabolic activities (Asharani *et al.* 2009). In this study, cisplatin (CDDP), an anti-cancer agent, was used as the positive control. As shown in Figs. 8a to 8d, it was found that there was a remarkable reduction in cell viability after induction of cisplatin agent, illustrating cytotoxicity of CDDP. Moreover, the cell viability steadily decreased when the concentration of CDDP

increased. Furthermore, the test results also indicate that all chemicals involved in the anti-microbial study were less cytotoxic to the fibroblast cells than the CDDP, *i.e.* there was no significant reduction in cell viability even at higher concentrations. In addition, Figs. 8b to 8d show that the overall cytotoxicity of different metal oxides increased in the order Ag₂O, nano-ZnO, and ZnO. Also, the higher the concentration of specific metal oxide, the higher the cytotoxicity. Nevertheless, it was confirmed that a small concentration of MF, MB, ZnO, nano-ZnO, and Ag₂O applied onto textile materials was safe to humans, even when it was in direct contact with the skin.

Mechanical Strength

Finishing processes of different kinds can impart different special and functional properties to fabrics. However, fibres may be damaged by mechanical processes and/or chemical agents, eventually causing a loss in strength. In this section, as shown in Table 4, tensile and tearing strength of cotton fabrics after treatment with different anti-microbial formulations were studied.

Table 4. Tensile and Tearing Strength of Anti-Microbial-Treated Cotton Fabric

Sample Symbol	Maximum Load (N)	Tearing Force (gf)
Control	315.0	917.6
M1	317.9	898.8
M2	306.3	928.3
M3	301.2	939.6
M4	297.1	945.5
M5	301.0	953.1
M6	303.7	933.1
M7	312.8	946.5
M8	304.2	1031.6
M9	302.7	1043.0
M10	292.6	1059.6
M11	304.1	1067.5
M12	300.6	1046.8
M13	306.6	1080.0

As presented in Table 4, breaking load of the control cotton fabric was 315.0 N, while the M1 specimen had a slightly higher breaking load. In general, it is assumed that tensile strength of an anti-microbial-treated specimen will be lower due to the acidity of MF-MB chemical mixtures, *i.e.* pH 5 as measured, which may weaken the fabric. In addition, the squeezing process during padding and the 140°C drying process also contribute to the loss of the strength of the fabric. However, MB is a self-cross-linking polyurethane dispersion that assists chemicals attachment to fibres. Therefore, during the grab test, it was more difficult to pull a specific width of the MF-MB-treated specimen together.

On the other hand, the overall breaking load of samples treated with MF-MB, in the presence of metal oxides, slightly decreased because a two-bath pad-dry method was used for treatment of cotton fabric, implying that the fabrics undergo padding and drying processes twice. Therefore, the mechanical process at a high temperature offset the improvement in fabric strength, contributed by application of MB. As shown in Table 4,

the decrease in breaking load of M8-M13 specimens also confirmed that the strength loss was mainly due to the padding and drying processes, rather than the acidic MF-MB chemical agents. Furthermore, the results show that the change in tensile strength was not related to the type of metal oxides applied.

Apart from the breaking strength, tearing strength of control and anti-microbial-treated specimens were also analyzed (Table 4). The Elmendorf tearing strength test determines the force required to propagate a single-rip tear starting from a cut in a fabric. In an instant, tearing force is applied to a single yarn during the test and then to the next yarn, after the first is broken; this is quite different from the grab test. Therefore, in tearing test, the glue-like MB applied on the fabric surface could not have helped the fabric withstand the tearing force. As presented in Table 4, the M1 specimen had slightly lower tearing strength compared with the control fabric, which might have been caused by the attack of acidic MF-MB chemical agents, *i.e.* pH 5 as measured, as well as the mechanical damage during padding and drying processes.

Table 4 also shows that the metal oxide catalyst might compensate for reduction in tearing strength caused by anti-microbial agents (M2-M7 specimens), especially when high concentration of metal oxide is used (M3, M5, and M7 specimens). This was probably due to the increased yarn friction, which helps resist yarn slippage. The more particles that are attached on the fabric surface or filled between the fibres, the higher the friction would be to resist yarn slippage. In addition, obvious enhancement in tearing strength occurred in M8-M13 specimens, which were not treated with acidic MF-MB chemical agents. Moreover, the results show that the change in tearing strength was irrespective of the type of metal oxides used.

CONCLUSIONS

1. The SEM images showed that the control fabric had a smooth and normal spiral structure, while MF-MB-treated specimens showed rougher and more wrinkled fiber surfaces. The irregularly shaped and sized metal oxide particles were agglomerated and unevenly attached to the cotton fabric.
2. The characteristic bands related to cellulose structure in cotton fibres were the hydrogen bonded OH stretching, the CO stretching, the CH stretching, and the CH wagging. In addition, a peak corresponding to the absorbed water molecules was observed. Moreover, it was confirmed that the MF-MB-treated fabric contained two medium sharp bands at 1670 and 1510 cm^{-1} , which were due to the benzene ring in aromatic compounds. Nevertheless, there was no new peak formed when the cotton fabric specimens were treated with metal oxide.
3. The cytotoxicity test confirmed that all chemicals involved in the anti-microbial study were less cytotoxic to the fibroblast cells than the CDDP and hence these chemicals, applied to textile materials, may be considered safe to humans, even when directly in contact with skin.
4. The anti-microbial activity of MF-MB-treated specimen against *E. coli* was contributed mainly by the MF agent, while only relatively small clustered metal oxide

particles provided an effective catalyzed reaction resulting in enhancement of anti-microbial activity. On the other hand, growth of *S. aureus* on the control fabric was only slightly inhibited, because of remnant H₂O₂, while anti-bacterial activity on MF-MB-treated specimen was enhanced, providing a slightly larger zone of inhibition. Moreover, fabrics finished with MF-MB in the presence of metal oxide exhibited better anti-microbial activity that was more effective against *S. aureus* than *E. coli*.

5. The MF-MB-treated specimen had slightly higher breaking load when compared with the control fabric due to the presence of self-crosslinking polyurethane dispersion. However, the glue-like MB did not help the fabric withstand the tearing force. Moreover, the overall breaking load of MF-MB-metal oxide-treated specimens was slightly decreased, which can probably be attributed to mechanical processing at high temperature. On the other hand, the metal oxide catalyst might compensate for reduction in tearing strength caused by anti-microbial agents, probably due to the increased yarn friction which helps resist yarn slippage.

ACKNOWLEDGMENTS

The authors wish to express their gratitude towards The Hong Kong Polytechnic University for financial assistance for this work.

REFERENCES CITED

- Abo-Shosha, M. H., El-Hosamy, M. B., Hashem, A. M., and El-Nagar, A. H. (2007). "A leaching type antibacterial agent in the easy-care finishing of knitted cotton fabric," *Journal of Industrial Textiles* 37(1), 55-77.
- AshaRani, P. V., Mun, G. L. K., Hande, M. P., and Valiyaveetil, S. (2009). "Cytotoxicity and genotoxicity of silver nanoparticles in human cells," *ACS Nano* 3(2), 279-290.
- Blake, D. M., Maness, P. C., Huang, Z., Wolfrum, E. J., and Huang, J. (1999). "Application of the photocatalytic chemistry of titanium dioxide to disinfection and the killing of cancer cells," *Separation and Purifications Methods* 28(1), 1-50.
- Chalmers, J. M., and Griffiths, P. R. (2002). *Handbook of Vibrational Spectroscopy*, Chichester, New York.
- Chen, C. Y., and Chiang, C. L. (2008). "Preparation of cotton fibers with antibacterial silver nanoparticles," *Materials Letters* 62(21-22), 3607-3609.
- Chen, H. L., and Burns, L. D. (2006). "Environmental analysis of textile products," *Clothing and Textile Research Journal* 24(3), 248-261.
- Chung, C., Lee, M., and Choe, E. (2004). "Characterization of cotton fabric scouring by FTIR ATR spectroscopy," *Carbohydrate Polymers* 58, 417-420.
- Daoud, W. A., Xin, J. H., and Zhang, Y. H. (2005). "Surface functionalization of cellulose fibers with titanium dioxide nanoparticles and their combined bactericidal activities," *Surface Science* 599, 69-75.
- Diebold, U. (2003). "The surface science of titanium dioxide," *Surface Science Report* 48(5-8), 53-229.

- El-Shishtawy, R. M., Asiri, A. M., Abdelwahed, N. A. M., and Al-Otaibi, M. M. (2011). "In situ production of silver nanoparticle on cotton fabric and its antimicrobial evaluation," *Cellulose* 18(1), 75-82.
- Fu, G. F., Vary, P. S., and Lin, C. T. (2005). "Anatase TiO₂ nanocomposites for antimicrobial coatings," *Journal of Physical Chemistry* 109(18), 8889-8898.
- Gao, Y., and Cranston, R. (2008). "Recent advances in antimicrobial treatments of textiles," *Textile Research Journal* 78(1), 60-72.
- Gorensek, M., and Recelj, P. (2007). "Nanosilver functionalized cotton fabric," *Textile Research Journal* 77(3), 138-141.
- Hadjiivanov, K. I., and Klissurski, D. G. (1996). "Surface chemistry of titania (anatase) and titania-supported catalysts," *Chemical Society Reviews* 25, 61-69.
- Hartzell-Lawson, M. M., and Hsieh, Y. (2000). "Characterizing the noncellulosic in developing cotton fibers," *Textile Research Journal* 70(9), 810-819.
- Heath, R. J., Rubin, J. R., Holland, D. R., Zhang, E., Snow, M. E., and Rock, C. O. (1999). "Mechanism of triclosan inhibition of bacterial fatty acid synthesis," *Journal of Biological Chemistry* 274(16), 11110-11114.
- Holt, K. B., and Bard, A. J. (2005). "Interaction of silver (I) ions with the respiratory chain of *Escherichia coli*: An electrochemical and scanning electrochemical microscopy study of the antimicrobial mechanism of micromolar Ag⁺," *Biochemistry* 44(39), 13214-13223.
- Ibrahim, N. A., Gouda, M., Hussein, Sh. M., El-Gamal, A.R., and Mahrous F. (2009). "UV- protecting and antibacterial finishing of cotton knits," *Journal of Applied Polymer Science* 112, 3589-3596.
- Ibrahim, N. A., Refaie, R., and Ahmed A.F. (2010). "Novel approach for attaining cotton fabric with multi-functional properties," *Journal of Industrial Textile* 40(1), 65-83.
- Ibrahim, N. A., Amr, A., Eid, B. M., Mohammed, Z.E., and Fahmy, H. M. (2012). "Poly (acrylic acid)/poly (ethylene glycol) adduct for attaining multifunctional cellulosic fabrics," *Carbohydrate Polymers* 89, 684-660.
- Ilić, V., Šaponjić, Z., Vodnik, V., Potkonjak, B., Jovančić, P., Nedeljković, J., and Radetić, M. (2009). "The influence of silver content on antimicrobial activity and color of cotton fabrics functionalized with Ag nanoparticles," *Carbohydrate Polymers* 78(3), 564-569.
- Karahan, H. A., and Özdoğan, E. (2008). "Improvements of surface functionality of cotton fibers by atmospheric plasma treatment," *Fibers and Polymers* 9(1), 21-26.
- Lewinski, N., Colvin, V., and Drezek, R. (2008). "Cytotoxicity of nanoparticles," *Small* 4(1), 26-49.
- Mahltig, B., Haufe, H., and Böttcher, H. (2005). "Functionalisation of textiles by inorganic sol-gel coatings," *Journal of Materials Chemistry* 15, 4385-4398.
- Morones, J. R., Elechiguerra, J. L., Camacho, A., Holt, K., Kouri, J. B., Ramirez, J. T., and Yacaman, M. J. (2005). "The bactericidal effect of silver nanoparticles," *Nanotechnology* 16(10), 2346-2353.
- Nakashima, T., Sakagami, Y., Ito, H., and Matsuo, M. (2001). "Antibacterial activity of cellulose fabrics modified with metallic salts," *Textile Research J.* 71(8), 688-694.
- Orhan, M., Kut, D., and Gunesoglu, C. (2008). "Improving the antibacterial activity of cotton fabrics finished with triclosan by the use of 1,2,3,4-butanetetracarboxylic acid

- and citric acid,” *Journal of Applied Polymer Science* 111(3), 1344-1352.
- Page, K., Palgrave, R. G., Parkin, I. P., Wilson, M., Savinc, S. L. P., and Chadwick, A. V. (2007). “Titania and silver-titania composite films on glass-potent antimicrobial coatings,” *Journal of Materials Chemistry* 17, 95-104.
- Parthasarathi, K., and Borkar, S. P. (2007). “Antibacterial and UV protection finishes of textiles by metal and metal oxide nano particles: A review,” *Colourage* 54(7), 43-45.
- Rajendran, R., Balakumar, C., Ahammed, H. A. M., Jayakumar, S., Vaideki, K., and Rajesh, E. M. (2010). “Use of zinc oxide nano particles for production of antimicrobial textiles,” *International Journal of Engineering, Science and Technology* 2(1), 202-208.
- Ramachandran, T., Rajendrakumar, K., and Rajendran, R. (2004). “Antimicrobial textiles - An overview,” (IELI) *Journal-Tx* 84(2), 42-47.
- Rezaei-Zarchi, S., Javed, A., Ghani, M. J., Soufian, S., Firouzabadi, F. B., Moghaddam, A. B., and Mirjalili, S. H. (2010). “Comparative study of antimicrobial activities of TiO₂ and CdO nanoparticles against the pathogenic strain of escherichia coli,” *Iranian Journal of Pathology* 5(2), 83-89.
- Shrivastava, S., Bera, T., Roy, A., Singh, G., Ramachandrarao, P., and Dash, D. (2007). “Characterization of enhanced antibacterial effects of novel silver nanoparticles,” *Nanotechnology* 18(22), 225103.
- Simonic, B., and Tomsic, B. (2010). “Structures of novel antimicrobial agents for textiles: A review,” *Textile Research Journal* 80(16), 1721-1737.
- Stewart, M. J., Parikh, S., Xiao, G. P., Tonge, P. J., and Kisker, C. (1999). “Structural basis and mechanism of enoyl reductase inhibition by triclosan,” *Journal of Molecular Biology* 290(4), 859-865.
- Suller, M. T. E., and Russell, A. D. (2000). “Triclosan and antibiotic resistance in *Staphylococcus aureus*,” *Journal of Antimicrobial Chemotherapy* 46(1), 11-18.
- Vigneshwaran, N., Kumar, S., Kathe, A. A., Varadarajan, P. V., and Prasad, V. (2006). “Functional finishing of cotton fabrics using zinc oxide-soluble starch nanocomposites,” *Nanotechnology* 17, 5087-5095.
- Vigneshwaran, N., Kathe, A. A., Varadarajan, P. V., Nachane, R. P., and Balasubramanya, R. H. (2007). “Functional finishing of cotton fabrics using silver nanoparticles,” *Journal of Nanoscience and Nanotechnology* 7(6), 1893-1897.
- Yazdankhah, S. P., Scheie, A. A., Høiby, E. A., Lunestad, B. T., Heir, E., Fotland, T. O., Naterstad, K., and Kruse, H. (2006). “Triclosan and antimicrobial resistance in bacteria: An overview,” *Microbial Drug Resistance* 12(2), 83-90.
- Zhang, F., Wu, X. L., Chen, Y. Y., and Lin, H. (2009). “Application of silver nanoparticles to cotton fabric as an antibacterial textile finish,” *Fibers and Polymers* 10(4), 496-501.
- Zhang, H., and Chen, G. (2009). “Potent antibacterial activities of Ag/TiO₂ nanocomposite powders synthesized by a one-pot sol-gel method,” *Environmental Science and Technology* 43(8), 2905-2910.

Article submitted: December 31, 2011; Peer review completed: June 23, 2012; Revised version received and accepted: July 9, 2012; Published: July 11, 2012.